

Screen Printable Electrochemical Capacitors on Flexible Substrates

Francisco J. Romero, Diego P. Morales, Almudena Rivadeneyra, Noel Rodriguez
Dept. Electronics and Computer Technology
University of Granada
Granada, Spain
e-mail: franromero@ugr.es, diegopm@ugr.es, arivadeneyra@ugr.es, noel@ugr.es

Markus Becherer
Institute for Nanoelectronics
Technische Universität München
Munich, Germany
e-mail: markus.becherer@tum.de

Abstract—This work presents a novel approach for the fabrication of Electrochemical Capacitors (ECs) based on the screen-printing of a commercial carbon-based conductive ink on flexible substrates. This technique enables the fast and cost-effective production of ECs with high flexibility and outstanding performance over bending states and voltage cycling, as demonstrated by means of cyclic voltammetry and galvanometric charge-discharge measurements. Despite the fact that the specific areal capacitances achieved are lower than the ones obtained using other carbon-based materials ($\sim 22 \mu\text{F}/\text{cm}^2$), the results show that, as soon as new screen-printable carbon-based pastes become available, this fabrication method will enable the mass production of ECs that can be attached to any surface as a conformal patch, as it is being required by a large number of the emerging technological applications.

Keywords- Carbon. Conductive ink. Electrochemical Capacitor. Flexible Electronics. Screen-printing. Specific Sapacitance.

I. INTRODUCTION

In recent years, flexible electronics has attracted the attention of many researches. This technology is expected to cause a disruption in the field of electronics devices, since it arises from the need to fulfill the demands required by novel technological applications, such as wearables or biomedical sensors, which cannot be addressed by means of the traditional silicon-based electronics [1]. Many of the advances in this context come with the emergence of new conductive and flexible materials. Examples of those are Carbon NanoTubes (CNTs) [2], graphene and its derivatives [3]-[5], or silver nanowires (AgNWs) and nanoparticles (AgNPs) [6][7]. Additionally, alternative fabrication processes enabling cost-effective processing on large flexible substrates are targeted. Those processes include printing technologies or laser treatment approaches, among others [8][9].

Thus, the combination of these two emerging lines of research has resulted in the development of many flexible electronics devices, including sensors [10][11], Radio Frequency Identification Tags (RFID) [12][13] and antennas [14][15]. Besides, apart from these latter, the flexible electronics progress is also requiring of flexible energy storage devices that, combined with energy harvesting

technologies, contribute to the development of self-powered devices [16].

Numerous studies have been conducted to examine different materials as electrodes for the fabrication of flexible Electrochemical Capacitors (ECs). Among them, carbon-based materials are the preferred to play this role for several reasons: *i*) exceptionally high surface area, *ii*) relatively high electrical conductivity and *iii*) acceptable cost [17]. Examples of materials studied so far are Laser-Induced Graphene (LIG) [18][19], reduced Graphene Oxide (rGO) [20] and single walled CNTs [21]. Many researchers agree that carbon-based electrodes will play an important role in the supercapacitor technology and that is why a big effort is being devoted to further optimizing its properties through doping [22] or surface treatments [23]. Besides, the performance of the electrochemical capacitors does not only rely on the material of the electrodes, but also on the electrolyte used. Therefore, it is also important to achieve a proper interaction electrode-electrolyte. Then, different acid/base/salt-Poly(Vinyl Alcohol) (PVA) gel electrolytes have been widely studied for this purpose, being the PVA/phosphoric acid (PVA/H₃PO₄) and the PVA/sulfuric acid (PVA/H₂SO₄) the ones which report the best performance [24][25].

In this contribution, we present a novel approach for the fabrication of flexible ECs based on the screen-printing of a commercial carbon-based electrically conductive ink using PVA/H₃PO₄ as electrolyte. We have opted for a 2D architecture, which consists of several InterDigital Electrodes (IDEs) arranged on a flexible substrate, since this configuration offers some advantages over the conventional designs, such as lower thicknesses and smaller distances between electrodes [16]. This paper is organized as follows. Section II describes the materials and methods used. Section III presents the performance of the presented ECs and, finally, Section IV addresses the main conclusions.

II. MATERIALS AND METHODS

A. Materials

Transparent polyester films for water-based inks with a thickness of 160 μm (from ColorGATE Digital Output Solutions GmbH, Hannover, Germany) were used as a flexible substrate for the fabrication of the capacitors. The screen-printing carbon-based paste used in this work, product

name: C-220, was provided by Applied Ink Solutions (Westborough, MA, USA). Both Poly(vinyl alcohol) (PVA, Mw 31,000-50,000, 98-99% hydrolyzed) and phosphoric acid (H_3PO_4 , product name: 1005731000) were acquired from Sigma-Aldrich (St. Louis, MO, USA). Electrical access to the capacitive devices was achieved using a silver nanoparticles (AgNPs) screen printable ink (LOCTITE® ECI 1010 E&C from Henkel AG, Düsseldorf, Germany).

B. Devices Fabrication

Figure 1 shows the scheme for the fabrication of the carbon-based flexible electrochemical capacitors. First, the in-plane interdigital electrodes were printed on the flexible substrate using a 90 Nylon threads per centimeter (T/cm) mesh with a FLAT-DX200 screen printing machine (from Siebdruck-Versand, Magdeburg, Germany), as shown in Figure 1a and 1b. The capacitive structure considered has the following dimensions (number of fingers N : 20, width W : 1 mm, spacing S : 1 mm, interspacing i : 1 mm and length L : 1 cm), which results in an effective area of 4 cm^2 , see Figure 1c. Following the manufacturer recommendations, the samples were dried at a temperature of $130 \text{ }^\circ\text{C}$ for 3 min to remove all residual solvent using a UF55 oven (from Memmert, Schwabach, Germany). Following the same screen-printing process, electrical contacts were printed using silver ink (Figure 1d), and the sample was dried afterwards again (this time at $120 \text{ }^\circ\text{C}$ for a duration of 15 min). Furthermore, the gel electrolyte was prepared by dissolving 1 g of PVA in 10 mL of de-ionized water (10 wt%) with stirring at $80 \text{ }^\circ\text{C}$ for 2 h using a VWR 12365-382 hot plate stirrer (from VWR International, Radnor, PA, USA). Once the PVA was completely dissolved, 1.2 g of H_3PO_4 was added to the solution and it was stirred for another hour [26]-[28]. The final homogeneous gel solution was drop casted ($\sim 1.5 \text{ mL}$) on the capacitive IDE structure covering all the effective surface area (Figure 1e). Finally, once the device is left standing overnight to remove the excess of water, the EC looks as shown in Figure 1f.

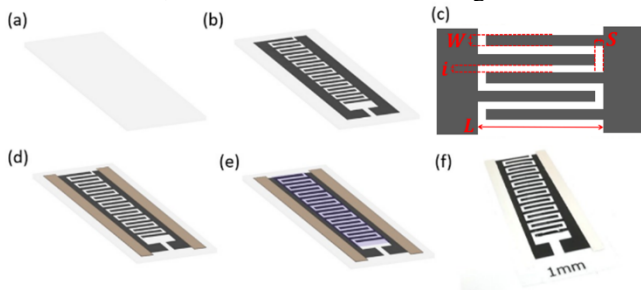


Figure 1. Schematic representation of the fabrication process of the flexible EC. (a) Flexible transparent substrate (thickness: $160 \mu\text{m}$). (b) Capacitive IDE structure screen-printed on the substrate. (c) Dimension of the interdigitally arranged electrodes (W : width, i : interspacing, L : length, S : spacing). (d) Silver electrical contacts screen-printed on each electrode. (e) PVA/ H_3PO_4 electrolyte drop-casted on top of the IDE structure (blue shadow color has been selected to make the electrolyte visible). (f) Real view of the EC presented in this work.

C. Characterization

Microscope pictures were obtained with a ZEISS AxioScope 5 (from Carl Zeiss AG, Oberkochen, Germany). The sheet resistances were measured through the four-point method at a constant Direct Current (DC) of $100 \mu\text{A}$ using a probe head from Jandel connected to a B2901A Keysight (Keysight Technologies, Inc., CA, USA) Source Measuring Unit (SMU). Cyclic Voltammetry (CV) and charge-discharge measurements at Constant Current (CC) were performed using a 2602B Keithley SMU from Tektronix Inc. (Beaverton, OR, USA). The impedance of the samples was obtained using the impedance analyzer 4294A (from Keysight Technologies, Inc., CA, USA). The performance of the devices as a function of the temperature was studied using the climate chamber VCL4006 (from Vötsch Industrietechnik GmbH, Balingen, Germany). A custom bending setup was built to perform the bending tests using a PD4-N5918M420 stepper motor together with a GPLE60 precision planetary gear (from Nanotec Electronic GmbH & Co. KG, Feldkirchen, Germany). All the measurement setup was automated using the software LabView 2017 (from National Instruments Corporation, TX, USA).

III. RESULTS AND DISCUSSION

Microscope images of the screen-printed electrodes are shown in Figure 2. On one hand, Figure 2a shows the printing resolution achieved. From the microscope images, it can be obtained that the average electrode width is $W = 1.168 \text{ mm}$, while its interspacing and separation are found to be $i = 0.892 \text{ mm}$ and $S = 0.902 \text{ mm}$, respectively, as a consequence of the paste spreading once it is deposited on the substrate. On the other hand, the porous nature of the carbon-based electrodes can be observed in Figure 2b. The sheet resistance of these conductive patterns is $503.6 \pm 74.4 \Omega/\text{sq}$.

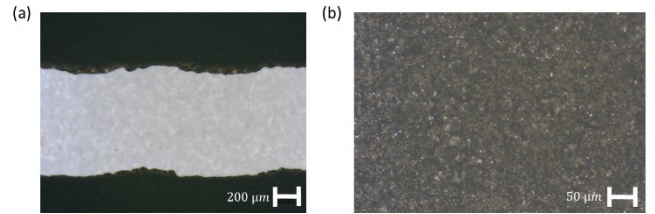


Figure 2. Microscope images of the screen-printed electrodes. (a) Interspacing between two consecutive electrodes (scale bar: $200 \mu\text{m}$). (b) Electrode surface (scale bar: $50 \mu\text{m}$).

First, the electrochemical performance of the ECs was investigated through Cyclic Voltammetry (CV). The experiments were conducted considering a potential window of $\Delta V = 1 \text{ V}$, from -0.5 V to $+0.5 \text{ V}$, at different scanning rates (20 mV/s , 50 mV/s , 90 mV/s , 120 mV/s), as shown in Figure 1a. It can be noted that the CV curves maintain the quasi rectangular shape over the increasing scan rates, indicating a good reversible Electrostatic Double-Layer Capacitive (EDLC) behavior [29]. From these curves, the capacitance can be calculated as follows:

$$C_{cv} = \frac{1}{2 \cdot \Delta V \cdot s} \cdot \left(\int_{-0.5}^{0.5} I(V) dV + \int_{0.5}^{-0.5} I(V) dV \right) \quad (1)$$

where ΔV is the potential window, s the scan rate and $I(V)$ the current response as a function of the voltage [20]. The results, depicted in Figure 3b, show an average capacitance of $\sim 12.5 \mu\text{F}$ ($\sim 3.1 \mu\text{F}/\text{cm}^2$). As seen, the capacitance does not suffer from a considerable decrease as the scan rate increases, which indicates a good interaction electrode-electrolyte [30].

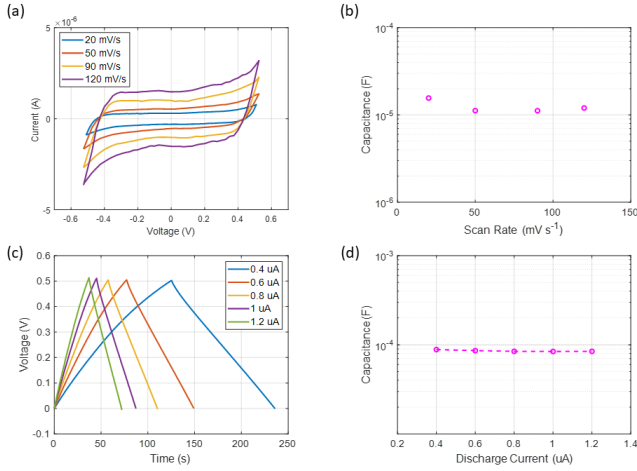


Figure 3. Evaluation of the specific capacitance of the ECs under different conditions. (a) Cyclic voltammetry curves at different scan rates. (b) Capacitance as a function of the scan rate extracted from the CV curves. (c) Galvanostatic charge-discharge curves at different constant currents. (d) Capacitance as a function of the discharge current extracted from the CC curves.

Galvanostatic charge-discharge measurements are also commonly used for the characterization of ECs. The resulting curves associated with these measurements are displayed in Figure 3c. In this case, the quasi triangular symmetric shape demonstrates a good charge propagation across the carbon electrodes and negligible internal resistances [31]. In the same way, these results can also be used to calculate the specific capacitance by the following equation:

$$C_{cc} = \frac{I}{dV/dt} \quad (2)$$

where I is the discharge current and dV/dt the slope of galvanostatic discharge curve [22]. In this case, the specific capacitance obtained is around $86 \mu\text{F}$ ($\sim 22 \mu\text{F}/\text{cm}^2$) with a slight decrease as the discharge current increases ($\Delta C/C_0 = 4.7\%$), see Figure 3d. This specific areal capacitance is similar to that obtained with other non-treated carbon materials [32][33].

The outstanding performance of the ECs under different bending conditions ($r = 1.25 \text{ cm}$, 0.75 cm and 0.5 cm) is demonstrated in Figure 4. It can be noted how the EC presents almost unchanged CC and CV curves for the different bending states, which would allow to use these ECs

in conformal applications with no effect on their electrochemical performance.

The electrochemical cycling durability of the ECs has also been studied. The results, displayed in Figure 5, have shown that the capacitors are able to retain their capacitance even after 1000 bending cycles ($\Delta C/C_0 < 1\%$). However, it can also be noticed how the rectangular shape of the CV curves is progressively deformed. This latter can be attributed to the appearance of reversible pseudocapacitive effects, indicating that an increasing number of continuous cycles boosts the electrosorption, redox and intercalation processes on the surface of the porous electrodes [20][34][35].

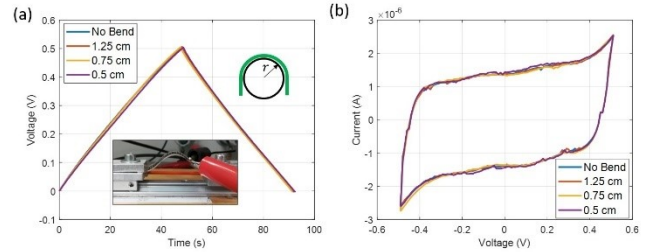


Figure 4. ECs performance under different bending conditions. (a) CC curves at the four different states ($I = 1 \mu\text{A}$). Inset shows a bent EC, while the diagram depicts the definition of bend radius. (b) CV curves for the four bending states considered ($s = 100 \text{ mV/s}$).

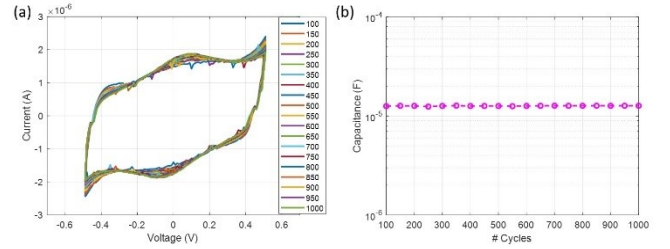


Figure 5. Cycle ability experiments. (a) CV curves obtained at the different cycles shown in legend. (b) Specific capacitance as a function of the number of cycles extracted from the CV curves.

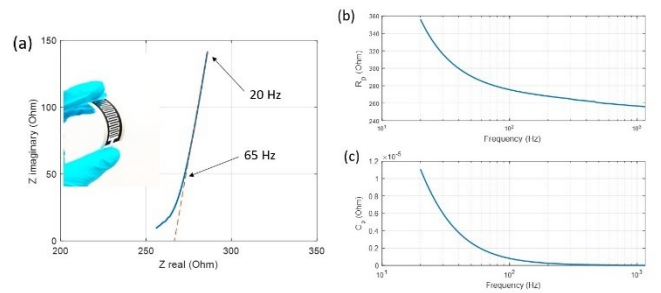


Figure 6. Electrochemical Impedance Spectroscopy (EIS) of the presented ECs. (a) Nyquist plot. (b) Equivalent resistance and (c) capacitance considering a simple model based on a $R||C$ circuit.

The ECs have been further investigated using a Nyquist diagram (Figure 6), which shows the capacitive behaviour of the presented ECs as a function of the frequency. At low frequencies, the imaginary part of the impedances against

the real one is almost linear (up to ~ 65 Hz), then a semicircle appears in the high frequency region indicating the transition between resistance and capacitance behaviours. It should also be noticed that, at this point, the curve faces the real axis at a $\sim 45^\circ$ angle, which is a common characteristic when a porous electrode is saturated with electrolyte [30][36][37]. Moreover, the interception with the real axis is associated with the Equivalent Series Resistance (ESR), which is estimated to be $\sim 250 \Omega$. Lastly, Figure 6b and Figure 6c show the behaviour of the analyzed ECs if we simplify its model to a capacitance in parallel with a resistance.

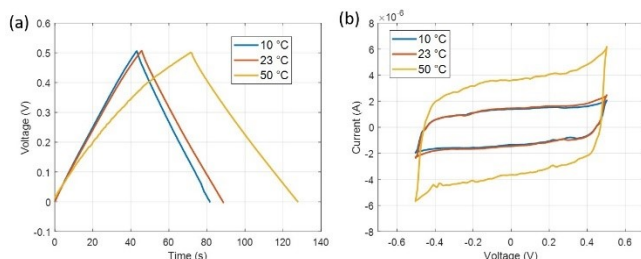


Figure 7. ECs performance under different bending conditions. (a) CC curves at the four different states. Inset shows a bent EC, while the diagram depicts the definition of bend radius. (b) CV curves for the four bending states.

Finally, the temperature effect on the performance of the ECs is represented in Figure 7. As demonstrated by both CC and CV experiments, the specific capacitance increases as the temperature increases, as it has been demonstrated for several electrode/electrolyte systems, such as rGO-PVA/H₃PO₄ [37], CNT-PC/TEABF₄ [38] and others [39]. This effect has been attributed to changes in the electrolyte, since an increase of the temperature possibly leads to the physisorption of the electrolyte ions [37][38].

IV. CONCLUSIONS

In summary, we report the fabrication of thin-film flexible electrochemical capacitors through the screen-printing of a carbon-based conductive ink on a flexible substrate. Using PVA/H₃PO₄ as electrolyte, the devices present good performance as ECDL capacitors, which has been demonstrated through cyclic voltammetry, charge-discharge experiments and electrochemical impedance spectroscopy. Although the specific capacitances obtained for this electrode material does not achieve those obtained with other carbon-based materials, further studies aim to treat the conductive ink in order to optimize its properties and increase the specific areal capacitance. It has been demonstrated that this method paves the way towards an alternative method for the large-scale and cost-effective fabrication of flexible electrochemical capacitors.

ACKNOWLEDGMENT

This work has been partially supported by the Spanish Ministry of Education, Culture and Sport (MECD) and the European Union through the pre-doctoral grant FPU16/01451, and its mobility program, the project TEC2017-89955-P and fellowship H2020-MSCA-IF-2017794885-SELFSENS.

REFERENCES

- [1] D. M. Sun, C. Liu, W. C. Ren, and H. M. Cheng, "A Review of Carbon Nanotube - and Graphene - Based Flexible Thin - Film Transistors," *Small*, vol. 9(8), 2013, pp. 1188-1205. DOI: 10.1002/sml.201203154.
- [2] E. Castillo *et al.*, "An optimized measurement algorithm for gas sensors based on carbon nanotubes: optimizing sensor performance and hardware resources," *IEEE Internet of Things Journal*, vol. 6(5), 2019, pp. 9140-9146. DOI: 10.1109/JIOT.2019.2928231.
- [3] H. Jang *et al.*, "Graphene - Based Flexible and Stretchable Electronics," *Advanced Materials*, vol. 28(22), 2016, pp. 4184-4202. DOI: 10.1002/adma.201504245.
- [4] G. Eda, G. Fanchini, and M. Chhowalla, "Large-area ultrathin films of reduced graphene oxide as a transparent and flexible electronic material," *Nature Nanotechnology*, vol. 3, 2008, pp. 270-274. DOI: 10.1038/nnano.2008.83.
- [5] F. J. Romero *et al.*, "In-Depth Study of Laser Diode Ablation of Kapton Polyimide for Flexible Conductive Substrates," *Nanomaterials*, vol. 8(7), 2018, 517. DOI: 10.3390/nano8070517.
- [6] D. Langley *et al.*, "Flexible transparent conductive materials based on silver nanowire networks: a review," *Nanotechnology*, vol. 24, 2013, 452001. DOI: 10.1088/0957-4484/24/45/452001.
- [7] W. Shen, X. Zhang, Q. Huang, Q. Xu, and W. Song, "Preparation of solid silver nanoparticles for inkjet printed flexible electronics with high conductivity," *Nanoscale*, vol. 6, 2014, pp. 1622-1628. DOI: 10.1039/C3NR05479A.
- [8] S. Khan, L. Lorenzelli, and R. S. Dahiya, "Technologies for Printing Sensors and Electronics Over Large Flexible Substrates: A Review," *IEEE Sensors Journal*, vol. 15(6), 2015, pp. 3164-3185. DOI: 10.1109/JSEN.2014.2375203.
- [9] H. Chang and H. Wu, "Graphene - Based Nanomaterials: Synthesis, Properties, and Optical and Optoelectronic Applications," *Advanced Functional Materials*, vol. 23(16), 2013, pp. 1984-1997. DOI: 10.1002/adfm.201202460.
- [10] F. J. Romero *et al.*, "Design, fabrication and characterization of capacitive humidity sensors based on emerging flexible technologies," *Sensors and Actuators B: Chemical*, vol. 287, 2019, pp. 459-467. DOI: 10.1016/j.snb.2019.02.043.
- [11] A. Salim and S. Lim, "Review of Recent Inkjet-Printed Capacitive Tactile Sensors," *Sensors*, vol. 17(11), 2017, 2593. DOI: 10.3390/s17112593.
- [12] J. F. Salmeron *et al.*, "Properties and Printability of Inkjet and Screen-Printed Silver Patterns for RFID Antennas," *Journal of Electronic Materials*, vol. 43(2), 2014, pp. 604-617. DOI: 10.1007/s11664-013-2893-4.
- [13] A. Albrecht, J. F. Salmeron, M. Becherer, P. Lugli, and A. Rivadeneyra, "Screen-Printed Chipless Wireless Temperature Sensor," *IEEE Sensors Journal*, 2019, 12011 - 12015. DOI: 10.1109/JSEN.2019.2940836.
- [14] Y. Goliya *et al.*, "Next Generation Antennas Based on Screen - Printed and Transparent Silver Nanowire Films," *Advanced Optical Materials*, vol. 7(21), 2019, 1900995. DOI: 10.1002/adom.201900995.

- [15] P. Lukacs, A. Pietrikova, J. Potencki, and G. Tomaszewski, "UWB Antenna Based on Nanoparticles of Silver on Polyimide Substrate," 38th International Spring Seminar on Electronics Technology (ISSE), May 2015, 15452268. DOI: 10.1109/ISSE.2015.7248031.
- [16] M. Beidaghia and Y. Gogotsi, "Capacitive energy storage in micro-scale devices: recent advances in design and fabrication of micro-supercapacitors," *Energy Environ. Sci.*, vol. 7, 2014, pp. 867-884. DOI: 10.1039/C3EE43526A.
- [17] A. G. Pandolfo and A. F. Hollenkamp, "Carbon properties and their role in supercapacitors," *Journal of Power Sources*, vol. 157(1), 2006, pp. 11-27. DOI: 10.1016/j.jpowsour.2006.02.065.
- [18] A. Lamberti, F. Clerici, M. Fontana, and L. Scaltrito, "A Highly Stretchable Supercapacitor Using Laser - Induced Graphene Electrodes onto Elastomeric Substrate," *Advanced Energy Materials*, vol. 6(10), 2016, 1600050. DOI: 10.1002/aenm.201600050.
- [19] Z. Peng, J. Lin, R. Ye, E. L. G. Samuel, and J. M. Tour, "Flexible and Stackable Laser-Induced Graphene Supercapacitors," *ACS Applied Materials and Interfaces*, vol. 7, 2015, pp. 3414-3419. DOI: 10.1021/am509065d.
- [20] Y. Chen, X. Zhang, D. Zhang, P. Yu, and Y. Ma, "High performance supercapacitors based on reduced graphene oxide in aqueous and ionic liquid electrolytes," *Carbon*, vol. 49, 2011, pp. 573 - 580. DOI: 10.1016/j.carbon.2010.09.060.
- [21] M. Kaempge, C. K. Chan, J. Ma, Y. Cui, and G. Gruner, "Printable Thin Film Supercapacitors Using Single-Walled Carbon Nanotubes," *Nano Lett.*, vol. 9(5), 2009, pp. 1872-1876. DOI: 10.1021/nl8038579.
- [22] Z. Peng *et al.*, "Flexible Boron-Doped Laser-Induced Graphene Microsupercapacitors," *ACS Nano*, vol. 9(6), 2015, pp. 5868-5875. DOI: 10.1021/acsnano.5b00436.
- [23] W. Wang *et al.*, "Tailoring the surface morphology and nanoparticle distribution of laser-induced graphene/Co3O4 for high-performance flexible microsupercapacitors," *Applied Surface Science*, In Press, 2019, 144487. DOI: 10.1016/j.apsusc.2019.144487.
- [24] Q. Chen *et al.*, "Effect of Different Gel Electrolytes on Graphene Based Solid-State Supercapacitors," *RSC Advances*, vol. 4, 2014, pp. 36253-36256. DOI: 10.1039/C4RA05553E.
- [25] W. Zhou *et al.*, "Flexible wire-like all-carbon supercapacitors based on porous core-shell carbon fibers," *J. Mater. Chem. A*, vol. 2, 2014, pp. 7250-7255. DOI: 10.1039/C3TA15280D.
- [26] D. He *et al.*, "Fabrication of a Graphene-Based Paper-Like Electrode for Flexible Solid-State Supercapacitor Devices," *Journal of Electrochemical Society*, vol. 165(14), 2018, pp. A3481-A3486. DOI: 10.1149/2.1041814jes.
- [27] J. Y. Shieh, S. H. Zhang, C. H. Wu, and H. H. Yu, "A facile method to prepare a high performance solid-state flexible paper-based supercapacitor," *Applied Surface Science*, vol. 313, 2014, pp. 704-710. DOI: 10.1016/j.apsusc.2014.06.059.
- [28] R. Singh and C. C. Tripathi, "Electrochemical Exfoliation of Graphite into Graphene for Flexible Supercapacitor Application," *Materials Today: Proceedings*, vol. 5(1), 2018, pp. 1125-1130. DOI: 10.1016/j.matpr.2017.11.192.
- [29] J. S. M. Lee, M. E. Briggs, C. C. Hu, and A. I. Cooper, "Controlling electric double-layer capacitance and pseudocapacitance in heteroatom-doped carbons derived from hypercrosslinked microporous polymers," *Nano Energy*, vol. 46, 2018, pp. 277-289. DOI: 10.1016/j.nanoen.2018.01.042.
- [30] G. A. M. Ali, L. L. Tan, R. Jose, M. M. Yusoff, and K. F. Chong, "Electrochemical performance studies of MnO2 nanoflowers recovered from spent battery," *Materials Research Bulletin*, vol. 60, 2014, pp. 5-9. DOI: 10.1016/j.materresbull.2014.08.008.
- [31] J. Luo *et al.*, "Integration of micro-supercapacitors with triboelectric nanogenerators for a flexible self-charging power unit," *Nano Research*, vol. 8(12), 2015, pp. 3934-3943. DOI: 10.1007/s12274-015-0894-8.
- [32] X. Zang *et al.*, "Evaluation of layer-by-layer graphene structures as supercapacitor electrode materials," *Journal of Applied Physics*, vol. 115, 2014, 024305. DOI: 10.1063/1.4861629.
- [33] J. J. Yoo *et al.*, "Ultrathin Planar Graphene Supercapacitors," *Nano Letters*, vol. 11, 2011, pp. 1423-1427. DOI: 10.1021/nl200225j.
- [34] J. Zhu *et al.*, "Multifunctional Architectures Constructing of PANI Nanoneedle Arrays on MoS₂ Thin Nanosheets for High-Energy Supercapacitors," *Small*, vol. 11(33), 2015, pp. 4123-4129. DOI: 10.1002/sml.201403744.
- [35] D. J. You *et al.*, "Redox-active ionic liquid electrolyte with multi energy storage mechanism for high energy density supercapacitor," vol. 7(88), 2017, pp. 55702-55708. DOI: 10.1039/C7RA10772B.
- [36] M. F. El-Kady, V. Strong, S. Dubin, and R. B. Kaner, "Laser Scribing of High-Performance and Flexible Graphene-Based Electrochemical Capacitors," *Science*, vol. 335(6074), 2012, pp. 1326-1330. DOI: 10.1126/science.1216744.
- [37] M. Wang *et al.*, "All-Solid-State Reduced Graphene Oxide Supercapacitor with Large Volumetric Capacitance and Ultralong Stability Prepared by Electrophoretic Deposition Method," *ACS Appl. Mater. Interfaces*, vol. 7(2), 2015, pp. 1348-1354. DOI: 10.1021/am507656q.
- [38] C. Masarapu, H. F. Zeng, K. H. Hung, and B. Wie, "Effect of Temperature on the Capacitance of Carbon Nanotube Supercapacitors," *ACS Nano*, vol. 3(8), 2009, pp. 2199-2206. DOI: 10.1021/nn900500n.
- [39] H. Y. Jung, M. B. Karimi, M. G. Hahm, P. M. Ajayan, and Y. J. Jung, "Transparent, flexible supercapacitors from nano-engineered carbon films," *Sci Rep.*, vol. 2, 2012, 773. DOI: 10.1038/srep00773.